Supplement to: Biomarker Proxy Records of Arctic Climate Change During the Mid-Pleistocene Transition from Lake El'gygytgyn (Far East Russia)

Kurt R. Lindberg[1,2], William C. Daniels[1], Isla S. Castañeda[1], Julie Brigham-Grette[1]

[1]University of Massachusetts Amherst, Amherst, MA, 01003, U.S.A.
[2]Now at: University at Buffalo, Buffalo, NY, 14260, U.S.A.

Correspondence to: Kurt R. Lindberg (kurtlind@buffalo.edu)

1 Introduction

This supplement contains Figures S1-S6 and associated discussion.

1.1 Leaf wax *n*-alkane distributions

The apolar fractions of the Lake El'gygytgyn lipid extracts contained *n*-alkanes with an average total concentration of 6.5 µg g sed^{-1} (n=149) and a high odd/even chain length ratio (Fig. S1). The Carbon Preference Index (Eq. S1) averages 3.6 (± 0.6 s.d.), indicating that the *n*-alkanes are sourced from plants and are not severely impacted by bacterial degradation.

Eq. S1. $CPI = \left[\frac{\Sigma(C25-C33)_{odd}}{\Sigma(C24-C32)_{even}} + \frac{\Sigma(C25-C33)_{odd}}{\Sigma(C26-C34)_{even}}\right] * 0.5$ (Bray and Evans, 1961)

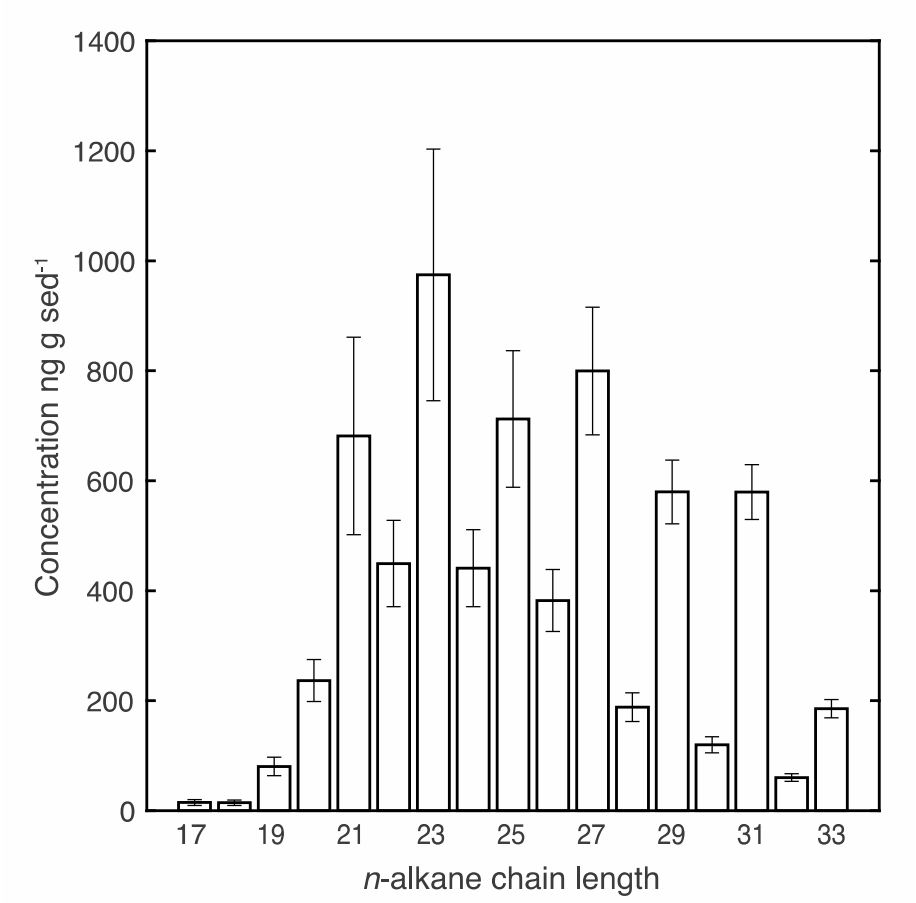

Figure S1: Bar plots of average leaf wax (*n*-alkane) concentrations in Lake El'gygytgyn samples from the MPT. Error bars represent the standard error of the mean (n = 149).

1.2 brGDGTs

Based on the branched GDGT concentrations, distributions, and isomerization, we conclude that the BayMBT calibration recently produced by Martinez-Sosa et al. (2021) provides the most reliable paleotemperature reconstruction from the GDGTs. First, the concentration of branched GDGTs (mean = 237 ng g sed^{-1}) is substantially higher than isoprenoid GDGTs (mean = 69 ng g sed^{-1}) over the MPT study interval (Fig. S2). The low concentrations of isoprenoid GDGTs, together with a number of biological confounding factors, limits the utility of the TEX_{86} paleothermometer at Lake El'gygytgyn (Daniels et al., in review).

In terms of brGDGT distribution, brGDGT IIIa is the most abundant, followed by the other acyclic compounds IIa and Ia (Figure S2). As discussed in the main text, hexamethyl compounds are more abundant than pentamethyl or tetramethyl compounds. The ternary diagram (Figure S5) illustrates how these samples compare to the global calibration samples. There is a strong contrast between the Lake El'gygytgyn samples and the global soil/peat samples of Naafs et al. (2017), which show a predominance of tetramethyl compounds. This is a strong indicator that the brGDGTs are sourced from within-lake production rather than from surrounding soils. The lakes calibration (Martinez-Sosa et al., 2021) has a large range in ternary space, with warmer samples represented by tetramethyl-dominant brGDGT distributions. The Lake El'gygytgyn data fall near the upper range of these samples, among other cold climate sites, and show some scatter from the main trend.

The analytical methodology employed here allows for separation of the brGDGT isomers. We find that the relative proportion of 6-methyl brGDGTs ranges from 0.1% to 33%, and averages 9% (Figure S3). Over the study interval, there is no apparent trend in the percentage of 6-methyl isomers. Weber et al. (2018) previously suggested that in lakes, the proportion of 6-methyl isomers is related to distinct GDGT producers residing in anoxic versus oxic strata depths of the water column. At Lake El'gygytgyn, there is geochemical evidence, based on the Mn/Fe ratio, indicating lake oxygenation has changed during the study interval, possibly impacting the assemblage of brGDGT producers. As such, we prefer to utilize the isomer specific MBT'_{5ME} index for the MPT temperature reconstruction, as it may relate to a narrower group of producers than indices incorporating 5-methyl and 6-methyl isomers.

Figure S4 shows the raw MBT'_{5ME} data, along with the three lakes-based calibrations discussed in the main text (Martinez-Sosa et al., 2021; Russell et al., 2018; Zhao et al., 2021). As can be seen, the temporal structure of the reconstructions is identical, as all three are based on the MBT'_{5ME} index. The most significant difference observed is the much higher magnitude of variability in the application of the Greenland Lake in-situ calibration of Zhao et al. (2021).

Figure S6 illustrates the relationship between the Lake El'gygytgyn MBT'_{5ME} record and orbital parameters during the MPT. In Fig. S6a, we observe that the temperature reconstruction tends to track the 41 kyr obliquity cycle, particularly in the older part of the interval. In Fig. S6b, we observe that summer insolation, dominantly controlled by the precession parameter, tracks many of the higher-frequency temperature changes. Notably, the terminations of MIS 32, 30, and 22 see increases in both the

Earth's tilt and the summer insolation. Some divergences between the temperature reconstruction and orbital variations are also evident. Most notably are the brief cold interval during MIS 23 which aligns with maxima in insolation and obliquity, and the return to glacial conditions during the upper portion of MIS 21 which also aligns with maxima in the orbital parameters.

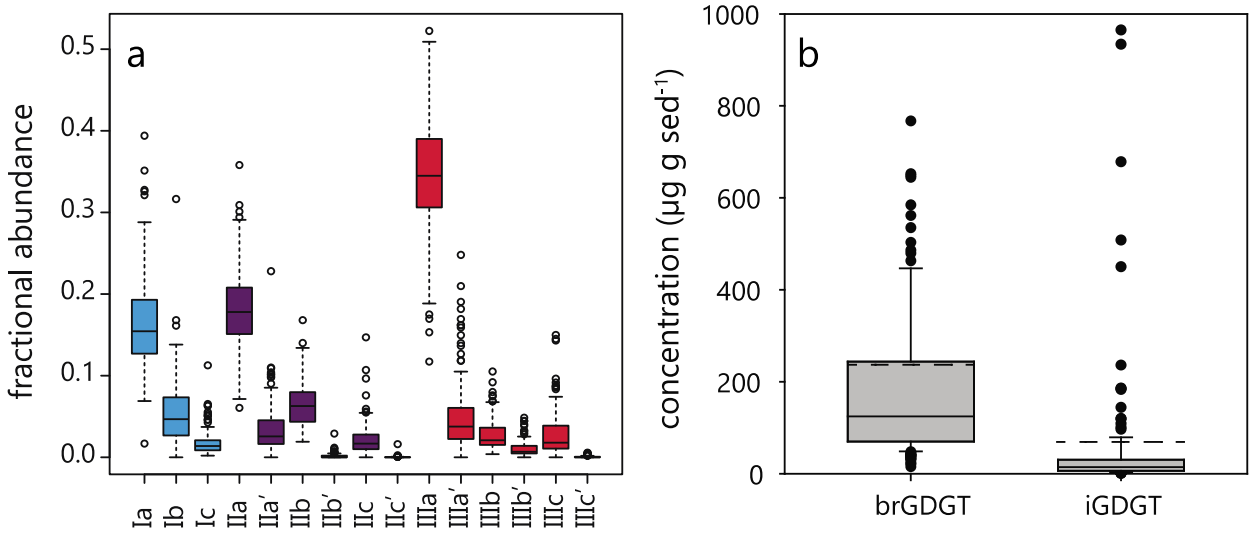

Figure S2: A) Boxplots of average brGDGT distributions in Lake El'gygytgyn samples from the MPT. Tetramethylated brGDGTs are shown in blue, pentamethylated brGDGTs in purple, and hexamethylated brGDGTs in red. The dominance of the 5-methyl isomers over the 6-methyl isomers (the brGDGT numbers Roman numerals and letters denoted with a prime symbol) is clear. B) Boxplots showing average concentrations of branched and isoprenoid GDGTs; brGDGT dominate Lake El'gygytgyn sediments. The solid line indicates the median value and the dashed line the mean. Two brGDGT outliers at 4213 and 4561 µg g sed^{-1} lie outside the scale of the Y-axis and therefore are not shown; nor is one iGDGT outlier at 3917 µg g sed^{-1}.

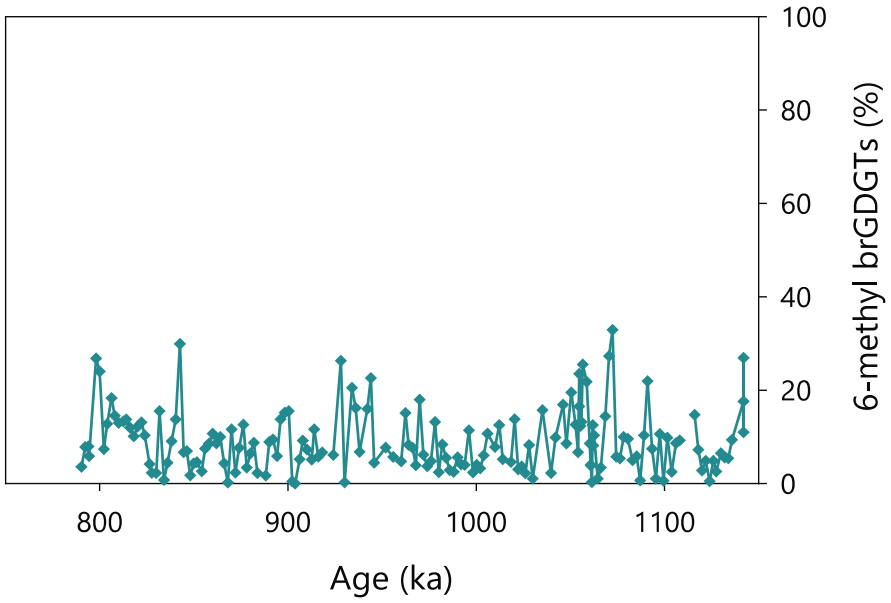

70

Figure S3: Fraction of 6-methyl brGDGTs at Lake El'gygytgyn during the MPT.

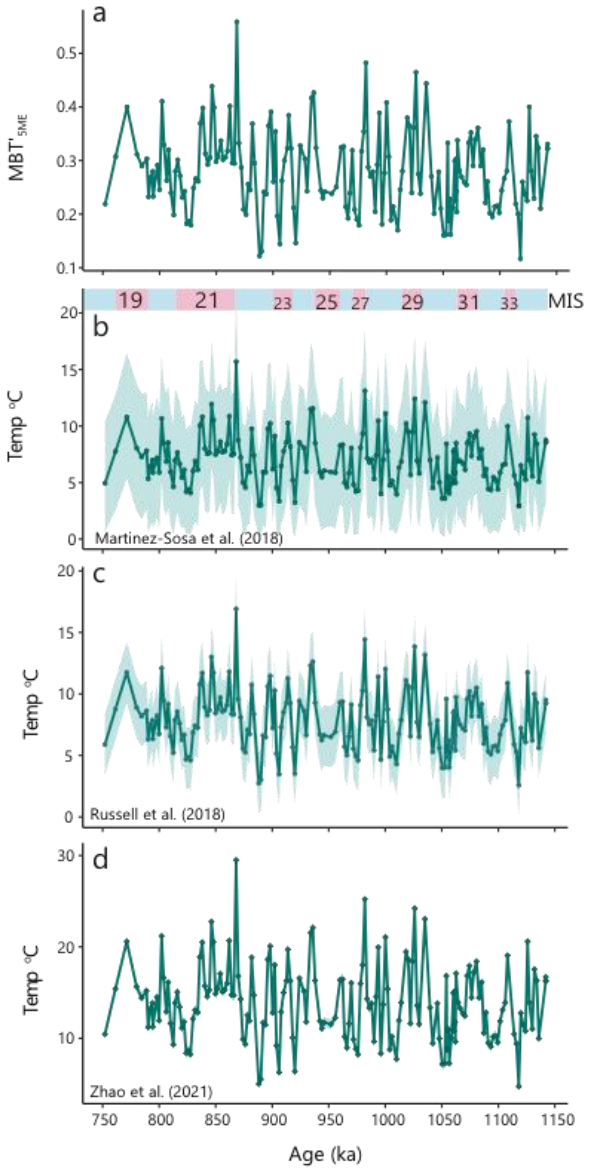

Figure S4

Figure S4: Application and comparison of different lacustrine-based calibrations for the Lake El'gygytgyn brGDGT temperature reconstruction. A) MBT'5ME results. B) Temperature of the months above freezing, based on the BayMBT calibration (Martinez-Sosa et al., 2021). C) Mean annual air temperature based on the African lakes calibration (Russell et al., 2018). Integrated water column temperature based on the in-situ calibration in Greenland lake (Zhao et al., 2021). Shaded areas represent the uncertainty associated with each calibration.

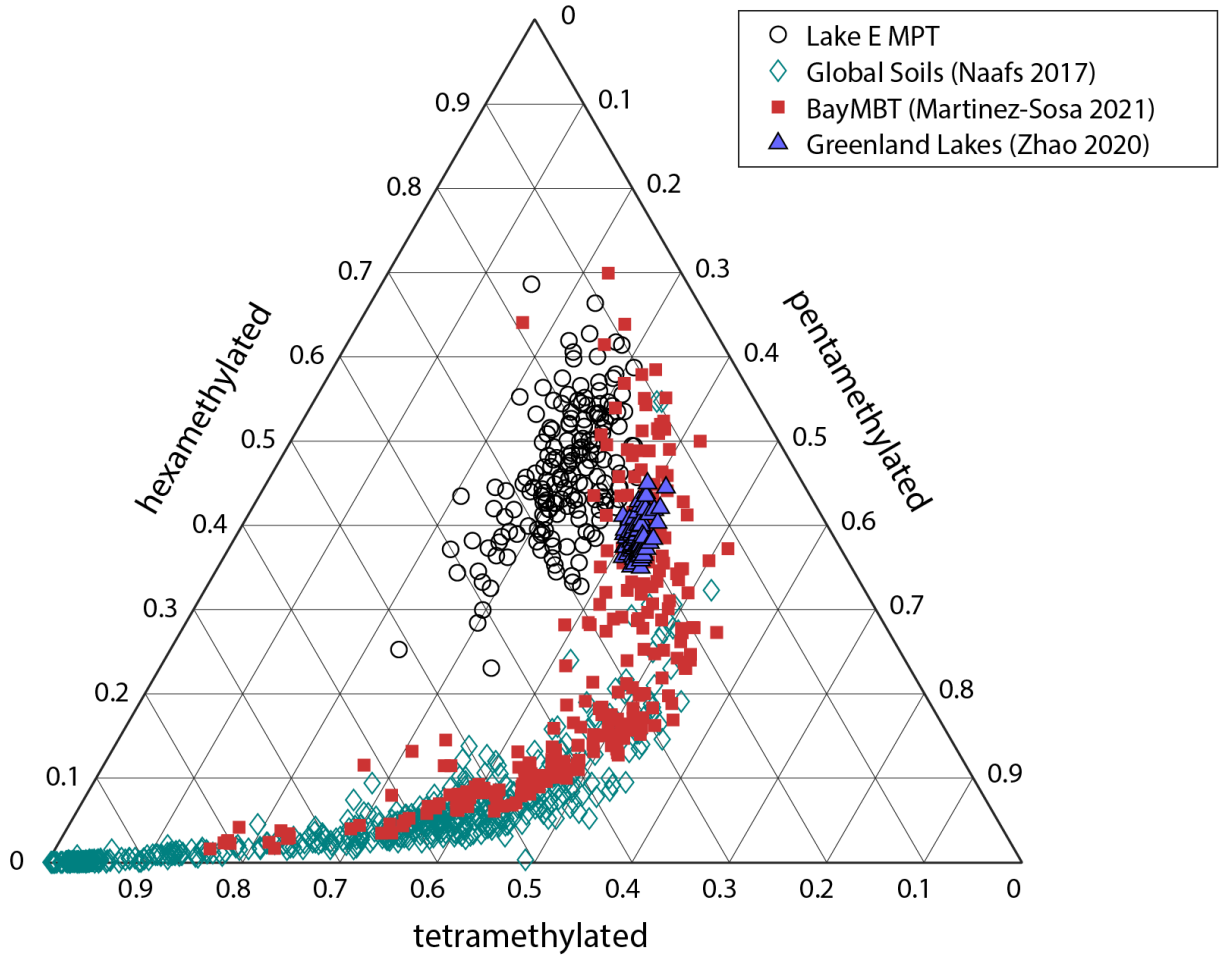

Figure S5: Ternary diagram showing the relative abundance of tetra-, penta-, and hexa-methylated brGDGTs in the Lake El'gygytgyn study interval (open black circles), and previously published calibration datasets including the BayMBT lakes dataset (red squares; Martinez-Sosa et al., 2021; Dang et al., 2018; Russell et al., 2018), the global soils dataset of Naafs et al. (2017), teal diamonds), and Lake 578 in Greenland (blue triangles, Zhao et al., 2021).

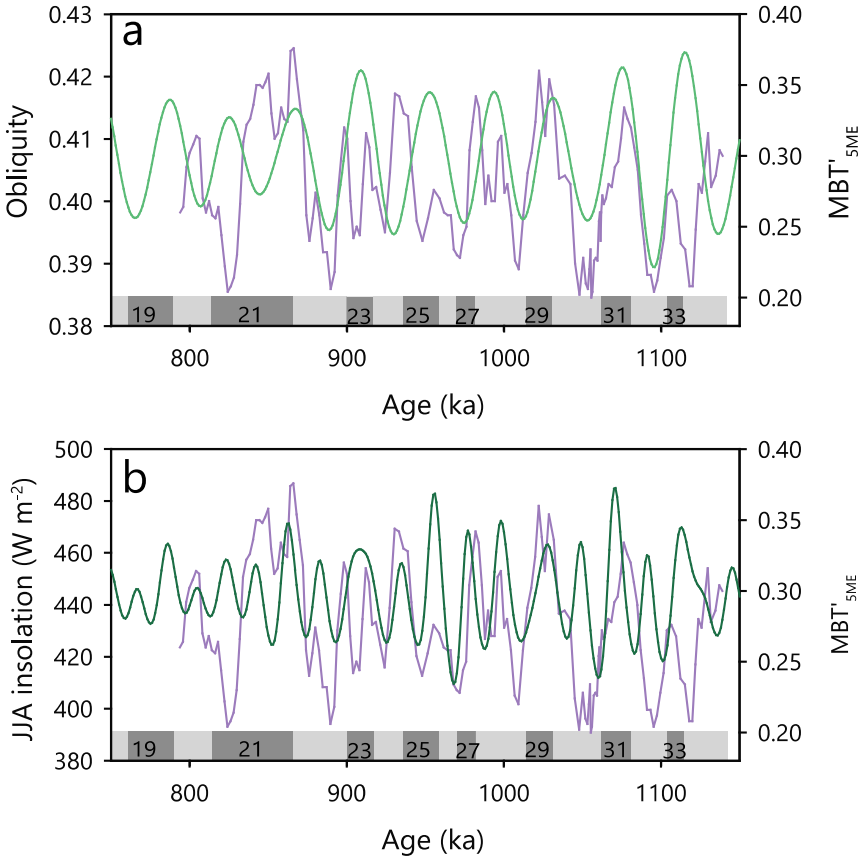

Figure S6: Comparison of the Lake El'gygytgyn brGDGT temperature reconstruction with astronomical forcings from Laskar et al. (2004). A) MBT'$_{5ME}$ results (purple) and obliquity (green). B) MBT'$_{5ME}$ results (purple) and insolation (June 21-Sept. 21) at 65° N latitude.

References:

Bray, E., and Evans, E.: Distribution of n-paraffins as a clue to recognition of source beds, Geochimica et Cosmochimica Acta, 22, 2-15, 1961.

Dang, X., Ding, W., Yang, H., Pancost, R. D., Naafs, B. D. A., Xue, J., Lin, X., Lu, J., and Xie, S.: Different temperature dependence of the bacterial brGDGT isomers in 35 Chinese lake sediments compared to that in soils, Organic Geochemistry, 119, 72-79, 2018.

Daniels, W., Castañeda, I., Salacup, J. M., Habicht, M. H., Lindberg, K., and Brigham-Grette, J.: Archaeal lipids reveal climate-driven changes in microbial ecology at Lake El'gygytgyn (Far East Russia) during the Plio-Pleistocene, Journal of Quaternary Science, in review.

Laskar, J., Robutel, P., Joutel, F., Gastineau, M., Correia, A., and Levrard, B.: A long-term numerical solution for the insolation quantities of the Earth, Astronomy & Astrophysics, 428, 261-285, 2004.

Martinez-Sosa, P., Tierney, J., Stefanescu, I. C., Crampton-Flood, E. D., Shuman, B. N., and Routson, C.: A global Bayesian temperature calibration for lacustrine brGDGTs, 2021.

Naafs, B. D. A., Inglis, G. N., Zheng, Y., Amesbury, M., Biester, H., Bindler, R., Blewett, J., Burrows, M., Del Castillo Torres, D., and Chambers, F. M.: Introducing global peat-specific temperature and pH calibrations based on brGDGT bacterial lipids, Geochimica et Cosmochimica Acta, 208, 285-301, 2017.

Russell, J. M., Hopmans, E. C., Loomis, S. E., Liang, J., and Sinninghe Damsté, J. S.: Distributions of 5-and 6-methyl branched glycerol dialkyl glycerol tetraethers (brGDGTs) in East African lake sediment: Effects of temperature, pH, and new lacustrine paleotemperature calibrations, Organic Geochemistry, 117, 56-69, 2018.

Weber, Y., Damsté, J. S. S., Zopfi, J., De Jonge, C., Gilli, A., Schubert, C. J., Lepori, F., Lehmann, M. F., and Niemann, H.: Redox-dependent niche differentiation provides evidence for multiple bacterial sources of glycerol tetraether lipids in lakes, Proceedings of the National Academy of Sciences, 115, 10926-10931, 2018.

Zhao, B., Castañeda, I. S., Bradley, R. S., Salacup, J. M., Gregory, A., Daniels, W. C., and Schneider, T.: Development of an in situ branched GDGT calibration in Lake 578, southern Greenland, Organic Geochemistry, 104168, 2021.